

ՀԱՅԱՍՏԱՆԻ ՀԱՆՐԱՊԵՏՈՒԹՅԱՆ ԳԻՏՈՒԹՅՈՒՆՆԵՐԻ ԱԶԳԱՅԻՆ  
ԱԿԱԴԵՄԻԱ Լ.Ա. ՕՐԲԵԼՈՒ ԱՆՎԱՆ ՖԻԶԻՈԼՈԳԻԱՅԻ ԻՆՍՏԻՏՈՒՏ

**ՇՈՒՇԱՆՅԱՆ ՌՈՒԶԱՆՆԱ ԱՐՍԵՆԻ**

ԱՌՆԵՏՆԵՐԻ ՈՐՈՇ ՕՐԳԱՆՆԵՐԻ ՄՈՐՖՈՖՈՒՆԿՑԻՈՆԱԼ  
ՓՈՓՈԽՈՒԹՅՈՒՆՆԵՐԻ ԳՆԱՀԱՏՈՒՄԸ ՍՈՒՐ ՀԻՊՈԲԱՐԻԿ  
ՀԻՊՕՔՍԻԱՅԻ ՊԱՅՄԱՆՆԵՐՈՒՄ

**Գ.00.09** – «Մարդու և կենդանիների ֆիզիոլոգիա» մասնագիտությամբ  
կենսաբանական գիտությունների  
թեկնածուի գիտական աստիճանի հայցման ատենախոսության

**ՍԵՂՄԱԳԻՐ**

ԵՐԵՎԱՆ– 2025

---

NATIONAL ACADEMY OF SCIENCES OF THE REPUBLIC OF ARMENIA  
INSTITUTE OF PHYSIOLOGY NAMED AFTER L. A. ORBELI

**SHUSHANYAN RUZANNA ARSEN**

ASSESSMENT OF MORPHOFUNCTIONAL CHANGES IN SOME  
ORGANS OF RATS UNDER ACUTE HYPOBARIC HYPOXIC  
CONDITIONS

**SYNOPSIS**

of dissertation for conferring of science degree of  
Candidate of Biological Sciences  
In the specialty of 03.00.09-Human and Animal Physiology

YEREVAN - 2025

Ատենախոսության թեման հաստատվել է Երևանի պետական համալսարանի գիտական խորհրդի նիստում:

Գիտական ղեկավար՝  
Պաշտոնական ընդդիմախոսներ՝

Կ.գ.թ., դոց. Աննա Ֆելիքսի Կարապետյան  
Կ.գ.դ., պրոֆ. Ռազմիկ Սարգսի  
Մխիթարյան  
Կ.գ.թ. Կարեն Վազգենի Սիմոնյան  
Երևանի Մ. Հերացու անվան պետական  
բժշկական համալսարան

Առաջատար կազմակերպություն՝

Ատենախոսության պաշտպանությունը կկայանա 2025 թ. մայիսի 29-ին, ժամը 13<sup>00</sup>-ին, ՀՀ ԳԱԱ Լ.Ա. Օրբելու անվան Ֆիզիոլոգիայի ինստիտուտում գործող ֆիզիոլոգիայի - 023 մասնագիտական խորհրդի նիստում (ՀՀ, 0028, ք. Երևան, Օրբելի եղբ. 22):

Ատենախոսությանը կարելի է ծանոթանալ ՀՀ ԳԱԱ Լ.Ա. Օրբելու անվան ֆիզիոլոգիայի ինստիտուտի գրադարանում և <http://www.physiol.sci.am> կայքում:

Սեղմագիրն առաքվել է 2025 թ. ապրիլի 29-ին:

023 մասնագիտական խորհրդի գիտական քարտուղար,  
կենսաբանական գիտությունների թեկնածու՝



Ն.Է. Թադևոսյան

---

The topic of the dissertation has been approved at the meeting of the Academic Council of Yerevan State University

Academic supervisor:

PhD in Biology, Assoc. Prof. Anna Feliks Karapetyan

Official opponents:

Dr.Sc., Assoc. Prof. Razmik Sargis Mkhitarian  
PhD in Biology Karen Vazgen Simonyan

Leading organization:

Yerevan State Medical University After Mkhitar Heratsi

The defense of the dissertation will be held on May 29, 2025 at 13:00, at the session of the specialized council 023 on Physiology, acting in the Institute of Physiology after L.A. Orbeli of NAS RA (22 Br. Orbeli str., Yerevan, 0023, Yerevan). L.A. Orbeli Institute of Physiology of NAS RA (22 Br. Orbeli str., Yerevan, 0023, RA).

The dissertation is available in the library of the Institute of Physiology after L.A. Orbeli NAS RA (Yerevan, 0023, Yerevan, 22, Br. Orbeli str. L.A. Orbeli Institute of Physiology of NAS RA and at: <http://www.physiol.sci.am>

The synopsis has been sent out on April 29, 2025.

Scientific secretary of 023 Specialized Council.

PhD in Biology



N.E.Tadevosyan

## INTRODUCTION

**Significance of the topic.** The brain and lungs rely heavily on a consistent oxygen supply for their structural and functional well-being. When faced with insufficient oxygen, these organs activate internal adaptation mechanisms, known as "hypoxic tolerance", to mitigate the potential harmful effects. This enables them to withstand acute and chronic hypoxic conditions caused by changes in atmospheric gas composition or physiological stress factors (Kumar et al., 2018).

Currently, it is estimated that 81.6 million people worldwide live and work under conditions of acute hypobaric hypoxia (HH), which refers to altitudes of 2100m and above sea level, indicating that this is an epidemiological problem (Hou et al., 2019). Accurate understanding of the physiological responses of the organism at high altitudes and mitigating organ damage caused by hypoxia is considered a global challenge today (Mallet et al., 2021). As is known, the main function of the lungs is gas exchange; therefore this is the organ that is directly responsible for supplying the body with oxygen. This is especially important under low atmospheric conditions. In general, the hypoxic state is considered a stress factor for the development of various pathological lung diseases, such as obstructive sleep apnea, acute hypoxic lung injury, asthma, atelectasis, obstructive pulmonary disease, and idiopathic pulmonary hypertension. Acute pulmonary hypoxia is associated with pulmonary arterial hypertension, epithelial dysfunction, edema formation, and inflammation (Araneda and Tuesta, 2012, Sargon, 2021, Mishra et al., 2015). The model of acute HH exposure is presented with a short duration of exposure (hours or days) (Arriaza et al., 2022), as a result of which among the most well-known diseases developing are acute mountain sickness, brain and lung edema, which are observed among non-acclimatized individuals and represent a great threat to their life and livelihood (Mehta et al., 2008). The main characteristic manifestation of cerebral edema is its cytotoxic and vasogenic edema, which has multiple causes including cellular, osmotic, and interstitial. Cerebral edema caused by these can develop not only as a result of HH but also due to brain tumors, traumatic injuries, ischemic stroke, infections, metabolic disorders or hypertension. Cellular or cytotoxic edema often occurs within minutes of hypoxic brain injury and affects its glial, neuronal, and endothelial cells. Cerebral edema can be asymptomatic and cause life-threatening complications, including cognitive, motor, and homeostatic dysfunction if preventive measures are not taken (Snyder et al., 2017; Nehring et al., 2024).

The main cause of the latter is perhaps the oxidative stress caused by hypoxia, which is considered one of the factors contributing to cognitive dysfunction, particularly memory deficit (Spanswick et al., 2011; Bocanegra et al., 2021). Oxidative stress is associated with many diseases of the central nervous system (CNS), accompanied by the damaging effects of oxygen free radicals (ROS) on cellular components such as proteins, phospholipids, and DNA (Upasana et al., 2021). Although little is known about the factors influencing the development of brain and lung edema, some biomolecules involved in oxidative stress are associated with inflammation, brain microcirculation, blood-brain, and alveolar-capillary barrier integrity disruption, and brain and lung endothelial dysfunction (Praneeti et al., 2018). From this point of view, a better understanding of the effect of oxidative stress and inflammatory mediators and cells in the development of hypoxic lung and

brain injury creates an opportunity to identify new target cells and/or mechanisms and develop possible preventive strategies based on them. Moreover, understanding the cellular and molecular mechanisms underlying the vulnerability of neural and alveolar cells to hypoxic injury may pave the way for the potential prevention and/or treatment of certain respiratory and neural diseases, including cerebrovascular diseases and pulmonary dysfunction (Motolese et al., 2015). Therefore, such a hypoxia-like model may be useful for elucidating the morphofunctional and biochemical features of the above mentioned disorders (Yamaoka et al., 1993).

**Research goals and tasks.** The aim of the current research is to investigate the effects of acute HH on the brain, lungs, and blood cells of rats through the analysis of morphofunctional alterations in the mentioned organs, as well as the key biomolecules associated with those changes.

Based on these objectives, the following research problems were defined:

1. To assess the histomorphological changes in distinct brain regions (hippocampus, cerebral cortex) under hypobaric hypoxic conditions.
2. To examine the roles of specific biomolecules implicated in oxidative stress in the pathogenesis of brain and lung edema development.
3. To determine the activity of mast cells and their released TNF- $\alpha$  activity involved in developing the inflammatory response in the brain and lungs under hypobaric hypoxic conditions.
4. To assess the alterations in certain peripheral blood cells under the influence of hypobaric hypoxia.
5. To investigate hypoxic lung damage by assessing the apoptotic activity in alveolar cells and the presence of fibrotic foci in lung tissue as well as to evaluate the apoptotic activity of neurons in the brain and examine the potential development of intracellular neurofibrillary tangles following hypoxic damage.
6. To determine the changes in the activity of some enzymes of the antioxidant defense system, such as catalase (CAT) and superoxide dismutase (SOD), as well as lactate dehydrogenase (LDH), as the most important enzyme of the anaerobic metabolic pathway.

**The scientific novelty of the study.** Through this work, the following key points were described and evaluated:

- For the first time, brain and lung damage under acute hypobaric hypoxic conditions has been thoroughly described and evaluated using a variety of cytological, histological, histochemical, immunohistochemical, biochemical, and fluorescence methods.
- The role of several important biomolecules in regulating oxidative stress, redox balance, and inflammatory reactions during acute hypoxic damage to the brain and lungs has been clarified.
- The presence of intracellular protein aggregations in the brain under acute hypobaric hypoxic conditions has been demonstrated, providing new insights into the neurodegenerative processes triggered by hypobaric hypoxia.

**Theoretical and practical importance of the work.** This research aims to explore the cellular and tissue-level processes triggered by brain and lung acute hypoxia. The findings could provide valuable insights into the mechanisms behind the formation of cerebral and pulmonary edema, aid in identifying potential biomarkers, and enhance our understanding of immune responses in the brain and lungs, as well as their interactions with the redox landscape in oxygen-dependent metabolic pathways under acute HH conditions. With the rising prevalence of neuroinflammatory, cerebrovascular, and respiratory diseases, this study is particularly timely. Additionally, the insights gained from this investigation could enrich curricula in neurobiology, stress physiology, and environmental physiology, serving as essential resources for education in these specialized fields. Moreover, the research could serve as a valuable resource for developing educational manuals and public health strategies in relevant fields, aimed at raising awareness among people living at high altitudes, mountaineers, and tourists.

**Work approbation.** The results of the work were presented in various conferences and reports that are listed below:

1. 1st International Conference for Young Neuroscientists “Brain and Neuroplasticity”. October 21-23, 2024, Georgia.
2. The 48th FEBS Congress, June 29-July 3, 2024, Italy.
3. The 47th FEBS Congress, July 8-12, 2023, France.
4. 9th International Youth Conference of YSU SSS, November 6-10, 2023, Yerevan.
5. Annual Conference of YSU Biology Research Institute, March 20-22, 2023, Yerevan, Armenia.
6. Oral report: The driving force of science. Neuroscience & Toxicology, May 26, 2023, Yerevan, Armenia.
7. Oral report: YSU, Faculty of Biology Scientific Reports Series, May 3, 2023. Yerevan, Armenia.

**Publications.** Based on the research results, 6 articles from which 4 ones were published in international peer-reviewed scientific journals and the 2 articles were published in the journals of HESC of the RA.

**Volume and structure of the dissertation.** The work is written on 120 pages and consists of an introduction, literary review, results of research, discussion, conclusions, and a list of literature containing 172 references. The work includes 41 diagrams and figures along with 9 tables.

## MATERIALS AND METHODS

**Materials & Methods.** Experiments were performed according to the directive 2010 (2010/ 63/EU) and approved by the local Bioethics Committee of Armenia. The experimental animals (male *Wistar* rats with 200-250g weight, n=40) were randomly divided into control (n=15) and HH groups (n=25), of which ten rats (n=5 from each study group) were used for biochemical and brain and lung water content analysis.

Animals were kept in standard laboratory conditions (1000m,  $\text{FiO}_2=20.1\%$ ,  $\text{pO}_2=131.4\text{mm Hg}$ ) for one week for acclimatization purposes under constant temperature ( $22\pm 2^\circ\text{C}$ ) and humidity (45-55%). All animals were maintained in a 12h light/dark cycled room and fed with free access to food and water *ad libitum*. Twenty five animals were exposed to acute HH for 24 hours in total at an altitude of 7620m (25000 feet,  $\text{FiO}_2=8.1\%$ ,  $\text{pO}_2=49\text{mm Hg}$ ) to mimic high altitude and simulate brain and lung edema formation. The animals of the experimental group were systematically removed from the decompression chamber every 6 hours for feeding, reoxygenation, and cleaning purposes. During this time, the animals were maintained under standard laboratory conditions for 1 to 2 hours before returning to the chamber. Each group, comprising five rats, was allocated two days to facilitate 24 hours of hypoxic exposure. Afterward, all rats were anesthetized using an intraperitoneal injection of ketamine hydrochloride (90 mg/kg) (Fahmy and Khair, 2022). The current data was selected according to the literature (Pena et al., 2012; Panahpour et al., 2014; Sarada et al., 2015; Sherman and Sladky, 2018). Numerous studies consistently support the use of 24-hour HH exposure to induce cerebral and pulmonary edema in both animal and human models. Notably, symptoms of mild to moderate acute mountain sickness, which is considered an early stage of high-altitude cerebral edema (HACE), can manifest soon after ascent and intensify over the next 24 to 72 hours, leading to vasogenic edema formation (Linlin et al., 2020; Turner, 2021; Yubo et al., 2023).

**Brain edema assessment.** After dissection, the left hemisphere of the brain samples ( $n=5/\text{group}$ ) was separated for brain water content (BWC) analysis, and the other hemispheres were used for biochemical study ( $n=5/\text{group}$ ). The tissue samples were measured to determine the wet weight by electronic balance ( $d=0.001\text{g}$ ), afterward, the samples were dried in a thermostatic oven at  $55^\circ\text{C}$  for 72h and then measured again for dry weight evaluation. Eliot's formula was used to estimate the BWC according to the following calculation:  $\text{water content (\%)} = [(\text{wet weight} - \text{dry weight}) / \text{dry weight}] \times 100\%$  (Guo et al., 2013).

**Lung edema assessment.** The wet/dry ratio was evaluated to demonstrate lung edema. The one lobe of the lungs ( $n=6/\text{group}$ ) was isolated and measured by electronic balance ( $d=0.001\text{g}$ ), to assess wet weight and then dried in an oven for 72 h to get the dry weight. According to the literature, the wet weight-to-dry weight ratio (W/D) was calculated as  $W/D = \text{wet weight} / \text{dry weight}$  (Liu et al., 2017).

**Histological analysis.** All animals from the control and experimental groups underwent histological assessment. The brain tissue samples were carefully dissected from the skulls and fixed in 10% formalin buffer for 48h. Likewise, lung samples from both control ( $n=6$ ) and experimental ( $n=16$ ) groups were processed for histological analysis. The lung tissue samples were carefully removed from the chest and fixed in 10% formalin buffer for 48h. Then, the sections were embedded with paraffin and sliced with microtome into 4-5 $\mu\text{m}$  thickness specimens. Afterward, the sections were dehydrated by descending concentrations of ethanol (96%, 90%, 80%, and 70%), dewaxed with xylene, and coverslipped with DPX.

**Immunohistochemical analysis.** To assess the TNF- $\alpha$ -expression following HH exposure, the IHC study was performed using an anti-TNF- $\alpha$  antibody (Abcam, 220210, Cambridge, UK). After draining off the blocking buffer from the slides, the primary antibody was applied and the slides

were maintained at 4°C overnight. Subsequently, the secondary HRP-conjugated antibody was used and the slides were incubated for 30 min at 37°C. For visualization, the diaminobenzidine chromogen (DAB, Abcam, UK) was used. The specimens were mounted with DPX and underwent light microscopy (B-293, OptikamB5 Digital Camera M-114, Italy). All captured images were recorded via Optika Liteview software with magnifications x100 and x400. The quantification of the cells (n=15/field) was performed via ImageJ software (NIH, Bethesda, USA).

**Mast cells (MCs) quantity assessment.** To determine the quantity and distribution of MCs, toluidine blue, and May-Grünwald Giemsa staining methods were used according to the literature (Rieger et al., 2013; Pena et al., 2024). Incidentally, both granulated and degranulated MCs (n=5/group) were detected. The number of MCs was counted per 15 observed fields under the light microscope (B-293, Italy).

**Oxidative stress assessment.** For determination of the total amount of nitric oxide (NO), the Griess reagent (Abcam, ab234044, Cambridge, UK) was applied according to protocol. The left cerebral hemispheres and one lobe of the lung were homogenized and centrifuged at 10,000g for 10 minutes to receive a supernatant. Then 100µl of samples were added to 10µl of enzyme cofactor by incubation with nitrate reductase. The measurement of optical density was carried out at 540nm by spectrophotometer at room temperature. Arginase (ARG) activity was measured as described by Roberts (Roberts, 1948), based on colorimetric determination. For that purpose, 0.05M MnCl<sub>2</sub> dilution (pH 9.5) was added to 0.5ml homogenate 5 ml of the arginine solution to give the final tissue concentrations indicated on the colorimetric analysis. The absorbance was measured with a spectrophotometer at 487nm. To evaluate the lipid peroxidation activity, the malondialdehyde (MDA) concentration in the brain and lung homogenates was analyzed according to the literature (Rael et al., 2004). The reaction with thiobarbituric acid reactive species (TBAS) was assessed spectrophotometrically at 532nm and the findings were visualized based on colorimetric assessment.

**Evaluation of antioxidant system activity.** Estimation of CAT activity was carried out by spectrophotometric method. For this purpose, brain and lung tissue samples were fixed in 0.9% NaCl solution to remove residual blood mass. A 10% homogenates of brain and lung tissues were then prepared by mixing it with a phosphate buffer (pH 7.4) and centrifuging at 4000g for 10 minutes. Following this, 1 ml of hydrogen peroxide (H<sub>2</sub>O<sub>2</sub>), 0.2 ml of potassium phosphate buffer, and 1 ml of ammonium molybdate were added to 0.2 ml of each sample. The optical density of the yellow complex formed by ammonium molybdate and hydrogen peroxide was measured spectrophotometrically at 374 nm at room temperature (Hamza and Hadwan, 2020). To determine SOD activity, a 10% tissue homogenate was centrifuged for 15 minutes (6000g), after which 1.8 ml of bicarbonate buffer (pH=10.55) and 0.1 ml of 1 % adrenaline. The optical density of the samples was measured with a spectrophotometer at room temperature at a wavelength of 347 nm, based on the determination of the maximum absorbance of the autoxidation intermediate of adrenaline. The optical density was measured for 3 minutes at 30 second intervals. The activity of SOD was evaluated according to the degree of inhibition of the autoxidation reaction rate of adrenaline expressed as % (Sirota, 2012).

LDH activity was determined based on the standard NADH assay (Hinman and Blass, 1981). For this, lung tissue samples were homogenized (10%) with the inactivation medium and centrifuged at 14000g for 15 minutes. Then, 2 ml of pyruvate dissolved in 2 ml of phosphate buffer (pH 7.5) along with 0.05 ml of NADH was added to each sample (0.1 ml). The quantitative reduction of NADH was measured using a standard spectrophotometric method at 340 nm. The mean optical density was recorded every 30 seconds over 3-5 minutes.

**Assessment of fibrosis.** A special Masson's Trichrome staining kit (DiaPath, Italy) was utilized according to the manufacturer's instructions to evaluate the degree of lung collagen deposition. The tissue samples underwent deparaffinization using xylene and were subsequently rinsed using distilled water. Then Weigert's iron hematoxylin was applied to the slides for 5 minutes. Subsequently, Biebrich Scarlet-acid fuchsin solution following 1% phosphomolybdic acid and Aniline blue solution were applied for 5 minutes, after which they were rinsed in distilled water and Acetic 1% acid solution for 2 minutes. The sections were then dehydrated in 96% alcohol, cleared in xylene, and mounted with DPX (Merck, Germany). To calculate the collagen deposition areas, the specimens underwent analysis by the ImageJ software (NIH, Bethesda, USA) as described in the literature (Chen et al., 2017). The regions with collagen fibril deposition were calculated as fibrotic areas (%).

**Evaluation of neurofibrillary tangles.** Congo red (CR) was used to visualize neurofibrillary tangles in tissue sections (Yakupova et al., 2019; Sarkar et al., 2020). Brain sections were deparaffinized and rehydrated, after which stained in 0.5% CR solution for 25min at room temperature, then rinsed in distilled water, alkaline alcohol solution (1ml of 1% sodium hydroxide diluted in 50% alcohol), dehydrated, and cleared with xylene, afterward mounted with DPX as described in the literature (Manickam et al., 2018). The counterstaining of the CR-positive cells was conducted for 30 observed fields under the light microscope (B-293, Italy).

**Evaluation of the presence of apoptosis.** Fluoro-Jade C (FJC) staining was used as a fluorescent histochemical marker for staining apoptotic cells and degenerating neurons in tissue slides (Schmued and Hopkins, 2000). The FJC staining procedure was conducted according to the manufacturer's instructions (TR-100-FJ, Biosensis, USA). After dewaxing, the brain slices were immersed in absolute then 70% alcohol for 5 min in each, and rinsed with distilled water. The slides were incubated in  $\text{KMNO}_4$  for 10 min at room temperature then washed with distilled water and immersed in 0.0001% FJC dye (0.01% stock solution diluted in distilled water) with DAPI solution for 30 min in dark conditions. Slides were washed twice, air-dried, and coverslipped with DPX. The images were observed with a fluorescent microscope (Euromex IS.3153 PLi/6, sCMEX-6 camera) under 485nm exciting light. The calculation of FJC-positive cells ( $n=35/\text{field}$ ) was conducted with the Image Focus Alpha software (Euromex Academy).

**Statistical analysis.** Sample Size Determination was performed using the Sample Size for One Sample, Continuous Outcome statistical analysis option using the following formula:  $n=(Z\sigma/E)^2$  where Z is the standard normal distribution value that reflects the confidence interval used (eg Z = 1.96 for 95%,  $\sigma$  is the standard deviation of the outcome variable and E is the desired margin of error (National Center for Health Statistics. Health, United States, 2005 with Chartbook on Trends in the Health of (Americans: Hyattsville, MD: 2005) Data from experiments were presented as

mean±SD for all methods used (unpaired, two-tailed). Whitney test using GraphPad software package, as well as two-way ANOVA - Tukey's Multiple Comparison test. Part of the data obtained was analyzed by one-way ANOVA (Kruskal-Wallis test) using Dunn's Multiple Comparison test. The statistically significant difference between the control and experimental groups was evaluated with values of \* $p < 0.05$ , \*\* $p < 0.01$  and \*\*\* $p < 0.001$ .

## RESULTS AND DISCUSSION

### 1. Histomorphological changes in different parts of the rat brain after acute hypobaric hypoxia

The control group specimens showed normal distribution of Nissl substance in the neurons with centrally allocated vesicular nuclei. The layer of neurons is arranged strictly and forms a dense layer containing CA1, CA2, and CA3 hippocampal subfields (Fig. 1 A, B, C). Histological sections of the brains of the control group rats also show intact layers of neurons in the cerebral (prefrontal) cortex (Fig. 1 D).

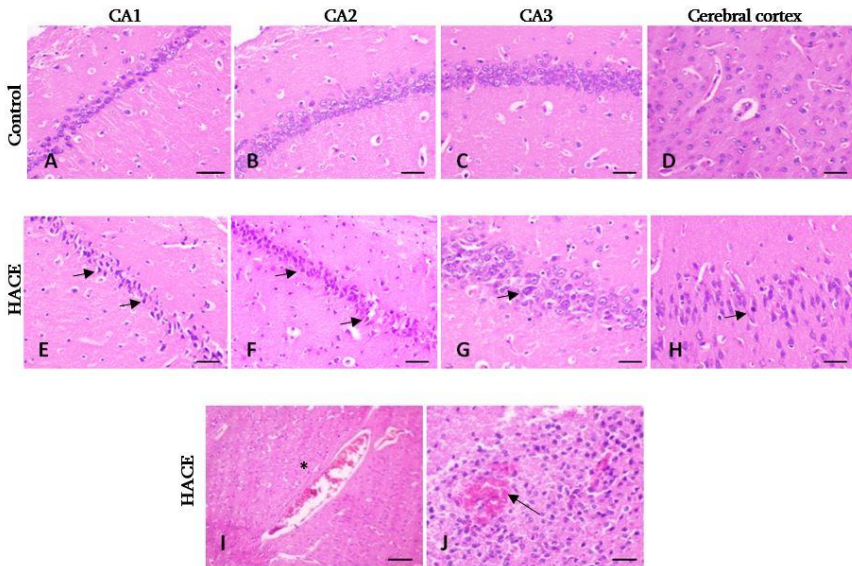


**Figure 1.** Histological photomicrographs of the CA1, CA2, and CA3 subfields of the hippocampus and cerebral cortex of control (A-D) and HACE group (E-J), (H&E staining, magnification x400, scale bar = 50 $\mu$ m). The short arrows indicate pyknotic, hyperchromatic cells within the hippocampus following hypoxic injury (E-H). Blood vessel congestion in the cerebral cortex (I, asterisk) is demonstrated in the HACE group with erythrocyte extravasation in the brain parenchyma (J, arrow), (magnification x400, scale bar = 50 $\mu$ m).

On the contrary, following the exposure to acute HH, there were determined remarkable changes in the brain, mainly the shrunken and hyperchromatic neurons with pyknotic nuclei in the prefrontal cortex and three cornu ammonis subfields of the hippocampus (Fig. 1E, F, G, H) with rearranged cells, and vacuolized neurocytes (edema). Additionally, congestion and dilated blood vessels were also observed in the rat's brain from the HACE group (Fig. 1 I). Some areas of the brain parenchyma were depicted with erythrocyte extravasation and microhemorrhages (Fig. 1 J).

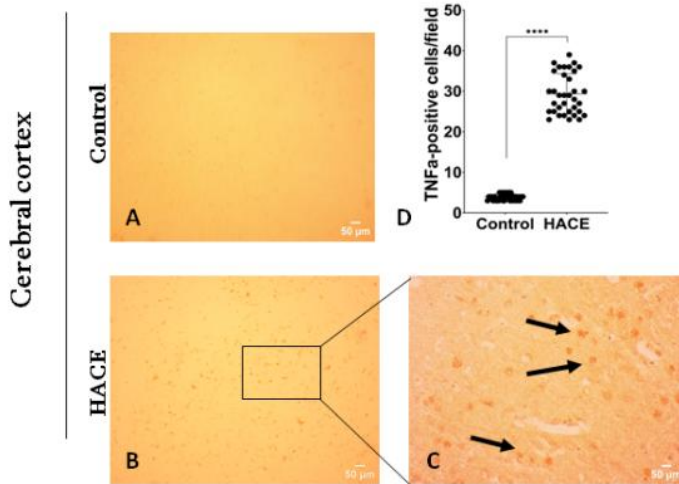


**Figure 2.** Histological microphotographs of the cerebral cortex of control (A), and HACE group (B, C), (magnification x100, scale bar=20μm, magnification x400, scale bar=50μm). Immunohistochemical study results showed TNF-α positive cells (arrows) per observed field (D), (\*\*\*\* $p < 0.0001$  compared with control according to Mann-Whitney test,  $n/\text{field}=15$ ).

The IHC analysis revealed significantly elevated TNF-α positive cells in the brain among HACE group animals in comparison to the control one (Fig. 2 A-C). Particularly, in the cerebral cortex the TNF-α positive cells were predominant (Fig. 2 D).

In parallel the average number of MCs also increased in response to hypoxic insult of the brain (Fig. 3F). The increase in the total number of granulated and degranulated MCs was particularly detected in the hippocampus (CA2 subfield), and dental gyrus (Fig. 3A-E).



mainly in the hippocampus (D-F), magnification x400, scale bar =50µm) in comparison to the control group (A-C), (magnification x400, scale bar=50µm, magnification x100, scale bar=20µm).

The CR staining reveals a high number of intracellular protein aggregations in the brain slice of the HACE group (Fig. 4). Namely, the CA1 region of the hippocampus demonstrated a marked increase of CR-positive cells ( $36.5\pm 2.63$ ), also in CA2 ( $22.3\pm 5.46$ ), CA3 ( $17\pm 5.48$ ) subfields and the cerebral cortex ( $15.92\pm 5.55$ ). This could be an adaptive response against acute hypobaric hypoxic exposure (Fig. 5).

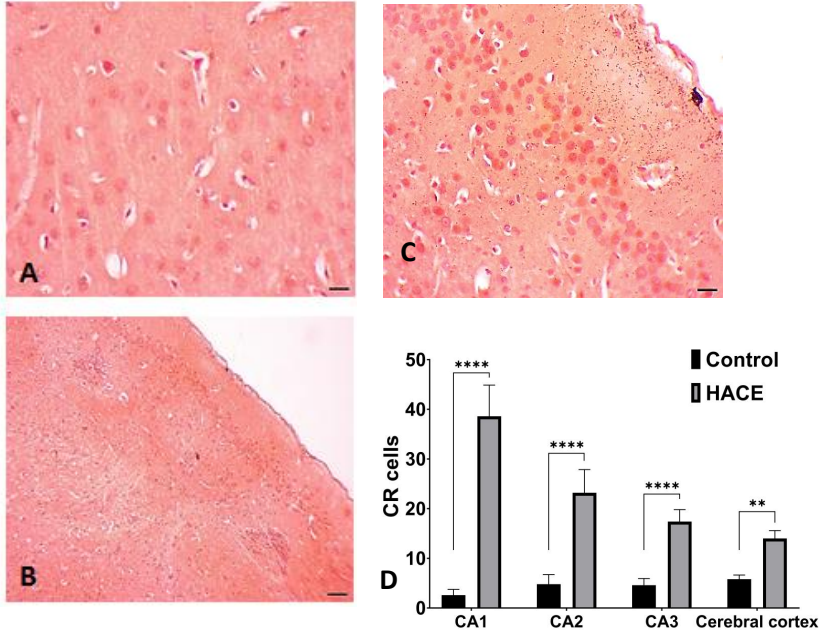


**Figure 5.** Histological photomicrographs showing CR-positive cells in the cerebral cortex. Several orange/red colored CR cells in the HACE group (C), (magnification x400) in comparison to the control group (A,B), (magnifications x100 and x400, scale bar =50µm). The number of CR-positive cells is significantly increased between the two studied groups (D), (\*\*\*\*p<0.0001, \*\*p<0.01 compared with control according to Tukey's test, n/field=30).

Next, the fluorescent analysis revealed prevalent FJC-positive cells in the HACE group that demonstrated neurodegeneration in the brain during exposure to HH (Fig. 6). Upon conducting a thorough histopathological examination, it was observed that hypobaric hypoxic exposure had brought about significant changes in the brain tissue.

Specifically, the neurons in the brain have undergone pyknosis and shrinkage. The examination also revealed a precise number of MCs and TNF- $\alpha$ -positive cells which are involved in the brain's adaptive response to inflammation.

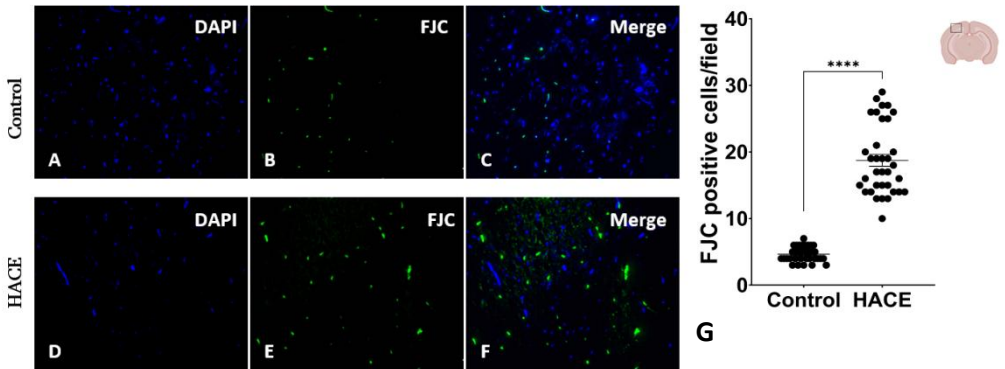


**Figure 6.** Histological photomicrographs showing DAPI-labeled (blue) and FJC-positive (green) cells represented in the cerebral cortex (scale bar = 50 $\mu$ m). There are a few degenerative neurons in the control group (A-C), while in the HACE group; those neurons are predominant (D-F). The number of FJC-positive cells is significantly increased between the two studied groups (G), (\*\*\*\* $p < 0.0001$  compared with control by Mann-Whitney test,  $n/\text{field} = 35$ ).

## 2. Biochemical assessment of the rat's brain following acute hypobaric hypoxia

Based on the received values of absorbance, the colorimetric assay demonstrated significant changes in concentrations among NO, ARG, and MDA. The biochemical findings are shown in Figure 7.

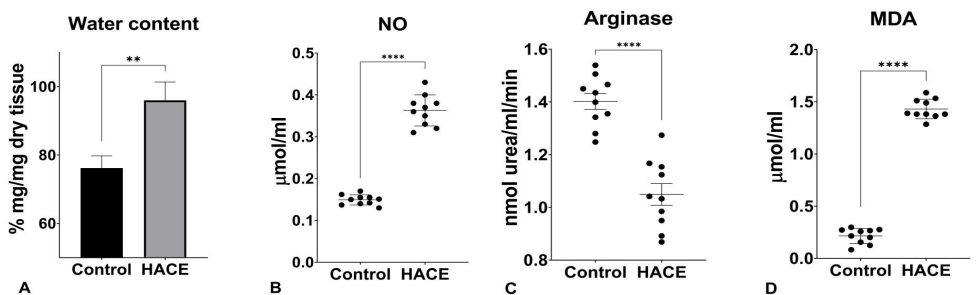


**Figure 7.** Brain water content analysis results (A). Values are presented as mean  $\pm$  SD and (\*\* $p < 0.01$  between control and HACE groups,  $n = 10$ ). Concentrations of Nitric Oxide (NO) (B), arginase (ARG) (C), and malondialdehyde (MDA) (D) represented as  $\mu\text{mol/ml}$  in response to HH, (\*\*\*\* $p < 0.0001$  show significant differences among groups based on Mann-Whitney test,  $n = 10$ ).

Sequentially, the rats exposed to HH showed significantly increased BWC ( $p < 0.01$ ) in comparison to control group animals (Fig. 7A), which was associated with BBB disruption and excess fluid accumulation in the brain parenchyma. This is possibly due to the increased activity of water channels, specifically with aquaporins (AQP4), and the activation of the NF- $\kappa$ B pathway. The observed changes of the MDA, ARG, and released NO activities show the redox imbalance occurred in the brain following acute HH exposure due to increased lipid peroxidation and ROS overproduction.

### 3. Histomorphological changes of the rat lung after acute hypobaric hypoxia

The lung tissue specimen from the control group (Fig. 8A) shows normal histomorphological architecture with alveolar epithelial cells and thin alveolar septa, while in the acute pulmonary edema group there was observed thickening of the alveolar walls with edematous changes (Fig. 8B, C, D). The interalveolar cavities were characterized by fluid accumulation (edema), additionally, dilated pulmonary vessels and erythrocyte extravasation was determined among alveolar beds (Fig. 8H, K, L).

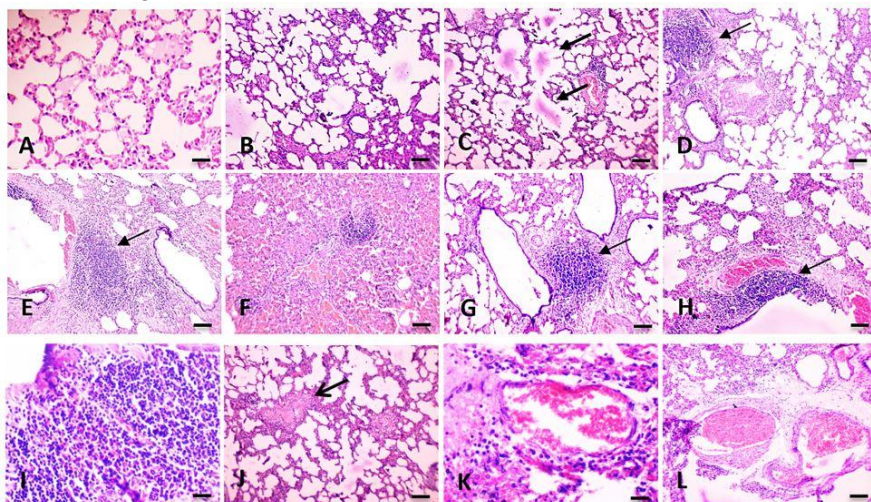


**Figure 8.** Histological photomicrographs of the lung tissue sample of the control group (A) that shows the normal structure of the alveoli septa with pneumocytes, and HAPE group (B-L), (H&E staining, magnification x400, scale bar = 150 $\mu$ m). Edematous fluid within the alveolar cavity (B, C, thick arrows), inflammatory infiltration among alveoli (D, F, G, I, thin arrows) and perivascular area (E, H, K), fibrosis with hyaline deposition in the alveoli lumen (D, J, stealthy arrow, magnification x600, scale bar =150 $\mu$ m). Microvascular injury with red blood cell extravasation and pulmonary vessel congestion shown in HAPE group sections (F, H, K, L, magnification x400, scale bar =150 $\mu$ m).

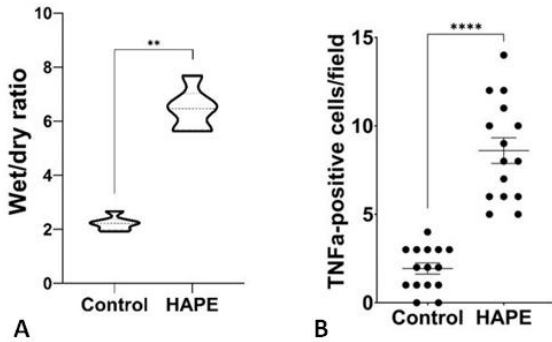


**Figure 9.** The wet/dry ratio of the lung (H), (\*\* $p < 0.01$  compared with control according to Mann-Whitney test,  $n = 6$ ). The TNF- $\alpha$ -positive cells in control and HAPE groups (I), (\*\*\*\* $p < 0.0001$  between two groups according to Mann-Whitney test,  $n/\text{field} = 15$ ).

The lung injury was also evidenced by the lung wet/dry ratio increase by 32% over the control group (Fig. 9A,  $p < 0.001$ ). Excess water content in the lung tissue after the hypoxic injury demonstrated the edematous changes of the organ due to increased permeability of the alveolar-capillary barrier. Noteworthy, the TNF- $\alpha$ -positive cells were predominant in the lung of the HAPE group outlining the onset of the inflammatory processes in the tissue after hypoxic exposure (Fig. 9B). The acute HH exposed group also revealed pulmonary tissue damage that was observed in the areas of collagen fibrils deposition increased by about 26% contrary to the control group (Fig. 10 G).

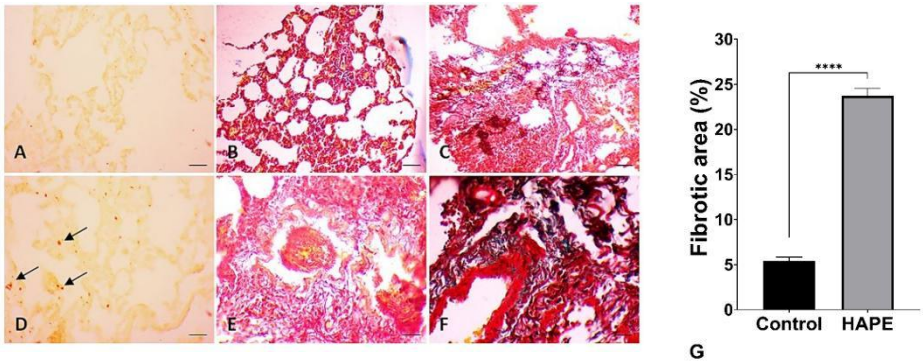


**Figure 10.** Histological photomicrographs of the lung tissue of control group sample (A), and HAPE group (D) showing TNF- $\alpha$ -positive cells (magnification x400, scale bar = 150  $\mu\text{m}$ ). Collagen fibers deposition among alveolar walls and pulmonary vessels of control (B, magnification x200), (E, magnification x400, scale bar=150  $\mu\text{m}$ ) and HAPE (C, magnification x200, scale bar=50  $\mu\text{m}$ ), (F magnification x400, scale bar=150  $\mu\text{m}$ ). The score of fibrotic area (%) in the HAPE group (G), (\*\*\*\* $p < 0.0001$  compared with control according to Mann-Whitney test,  $n/\text{field} = 30$ ).

Contrary to the control group, the lungs of the HAPE group also exhibited an elevated number of MCs that significantly increased after hypoxic injury of the tissue (Fig. 11G,  $p < 0.001$ ). The MCs were mostly distributed among the alveolar septa and within the bronchioles (Fig. 11A-F).

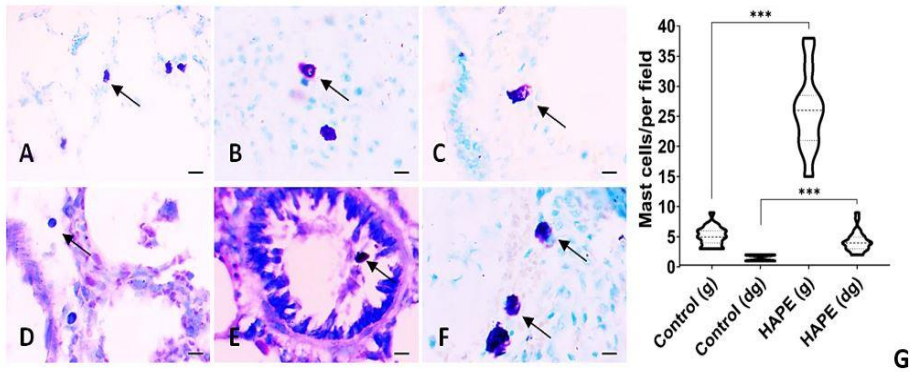


**Fig. 11.** Histological photomicrographs showing granulated MCs in the lung tissue of pulmonary edema group **A, B** (thick arrows, Toluidine blue staining, magnification  $\times 400$ , scale bar =  $150\mu\text{m}$ ), **D, E** (thick arrows, Giemsa staining, magnification  $\times 400$ , scale bar =  $150\mu\text{m}$ ). The degranulated MCs demonstrated in the lung of HAPE group specimens, **(C)**, (Toluidine blue staining, magnification  $\times 400$ , scale bar =  $50\mu\text{m}$ ), and **(F)** (Giemsa staining, magnification  $\times 400$ , scale bar =  $50\mu\text{m}$ ), **(G)**, granulated (g) and degranulated (dg) MCs in the studied groups (data presented as mean  $\pm$  SD, (\*\*\*)  $p < 0.001$  compared with control according to one-way ANOVA (Kruskal-Wallis test) using Dunn's multiple comparisons test,  $n/\text{field} = 25$ ).

These findings suggest that MCs play a role in the development of pulmonary edema, as evidenced by a significant increase in both granulated and degranulated cells. The degranulation of MCs may lead to the release of histamine and  $\text{TNF-}\alpha$ , which can contribute to the disruption of the alveolar-capillary barrier integrity and be accompanied by water leakage into the lung tissue.

#### 4. Biochemical assessment of the rat's lung following acute hypobaric hypoxia

The biochemical analysis of the studied group showed that in contrast to the control group animals, the HAPE group showed a significant decrease in NO level and an increase in ARG after hypobaric hypoxic exposure (Fig. 12A, B,  $p < 0.05$ ). Interestingly, the level of MDA following hypobaric hypoxic injury was dropped (Fig. 12C). Considerably, the NO plays a significant role in the development of high-altitude pulmonary edema (HAPE) by acting as a vasodilator and oxidative stress marker. Additionally, the changes in ARG levels support the idea that HAPE may be related to the disruption of redox homeostasis and the changes in the NO-synthesis pathway. Furthermore, acute exposure to high altitude changed the redox balance, leading to a decrease in

NO and an increase in ARG that considerably contributed to edema formation and the activation of ROS production.

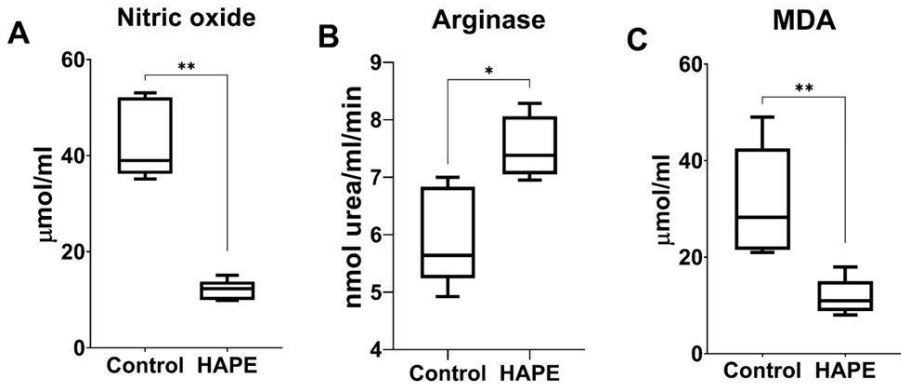


**Fig. 12.** Concentrations of Nitric Oxide (NO) (A), arginase (ARG) (B), and malondialdehyde (MDA) (C) represented as  $\mu\text{mol/ml}$  in the control and HAPE groups (\* $p < 0.05$ , \*\* $p < 0.01$  show significant differences among groups based on Mann-Whitney test,  $n = 5/\text{group}$ ).

Acute HH has also been observed to activate the MCs to degranulate and increase  $\text{TNF-}\alpha$  expression. High altitude has been found to cause alveolar-capillary barrier disruption, juxtaposed with inflammation and oxidative damage of the lungs. These also have been evidenced by the wet/dry ratio increase after acute HH along with the histopathological findings supporting the idea that these changes contribute to lung tissue remodeling and pulmonary edema development under conditions of the high-altitude environment.

## 5. Assessment of the changes in the antioxidant system in the rat's brain and lung following acute hypobaric hypoxia

The toxic effects of oxygen are usually mediated by its metabolites, such as superoxide anion, hydroxyl radicals, hydrogen peroxide, and active (singlet) oxygen. In lung cells, several endogenous enzyme systems (including superoxide dismutase, catalase, and glutathione oxidase) protect cell membranes from these metabolites (Bonuccelli et al., 1993).

The final chapter of the study examines the effects of acute HH on brain and lung antioxidant enzymes, specifically SOD, CAT, and LDH activity. The results of biochemical analysis of these enzymes are given in Table 1.

**Table 1.** Changes in superoxide dismutase (SOD), catalase (CAT), and lactate dehydrogenase (LDH) activity in control and HACE and HAPE groups respectively, \*\*\* $p < 0.001$ , \*\* $p < 0.01$ , \* $p < 0.05$ , *ns*-not significant (n/group=5)

Antioxidant defense system	Experimental groups			
	Control	HACE	Control	HAPE
SOD ( $\mu\text{mg}$ )	0.120 $\pm$ 0.01	0.690 $\pm$ 0.03**	0.269 $\pm$ 0.22	0.191 $\pm$ 0.09*
CAT ( $\mu\text{kat/mg}$ )	2.252 $\pm$ 0.27	1.677 $\pm$ 0.18*	5.456 $\pm$ 1.5	2.424 $\pm$ 1.9*
LDH ( $\mu\text{mol NADH /min x mg tissue}$ )	0.386 $\pm$ 0.02	0.396 $\pm$ 0.03 <sup>ns</sup>	0.165 $\pm$ 0.01	0.495 $\pm$ 0.04***

The results show that after exposure to hypoxia, the activity of catalase and SOD increased in the brain compared to the control group, which indicates the presence of active peroxidation processes in this organ, while the opposite phenomenon was observed in the lungs with decreased CAT and increased SOD activity. The stability of LDH results indicates that the brain can rapidly transition to anaerobic glycolysis when necessary. This underscores the importance of lactate not only as a metabolic byproduct but also as a vital source of energy for neuronal function. In the present study, LDH activity exhibited no significant changes in the brain following exposure to HH; however, an increase in its activity was observed in the lungs. This also indicates a systemic failure of the organ to manage oxidative stress, which likely resulted in impaired respiratory chain function in the mitochondria and reduced ATP synthesis, linked to elevated levels of LDH in the lungs. Nevertheless, these differential responses of the lungs and brain to hypoxia highlight the specific adaptations of these organs to conditions of oxygen deficiency.

### CONCLUSIONS

1. The exposure to acute hypobaric hypoxia was accompanied by karyopyknosis and vacuolation of the cells of the prefrontal cortex, and pyknotic changes in the hippocampal subfields along with vascular hyperemia, while the lungs displayed evidence of hemorrhages, inflammatory infiltrates, and erythrocyte extravasation.
2. Oxidative stress within the brain was correlated with a 72% reduction in NO levels, a 34.3% decrease in MDA, and a 35.7% increase in ARG activity. In the lungs, NO and MDA levels diminished by 37.9% and 22.5%, respectively, while ARG activity increased by 20.2%. These findings indicate a significant disturbance in the redox balance within these organs.
3. The number of TNF- $\alpha$ -positive cells and FJC-positive apoptotic neurons in the brain and lungs increased 4 times, and the number of mast cells in the brain and lungs increased 10 and 5 times, respectively. After acute HH exposure, the number of CR-positive neurons in the brain increased in the CA1, CA2, and CA3 regions of the hippocampus, as well as in the cortex.

4. An analysis of peripheral blood revealed a 33.7% increase in the number of lymphocytes, while the count of neutrophils declined by 30%.
5. The dry-to-wet weight ratio for both the brain and lungs increased by 15.7% and 34.4%, respectively, indicating the presence of edema formation in these organs. Furthermore, there was a notable accumulation of collagen fibers in the lungs, as evidenced by a 25.6% increase in fibrotic areas.
6. The activity levels of SOD, MDA, catalase, and LDH were changed in the brain and lungs which indicates a possible disruption in lipid peroxidation and glucose metabolism in these organs.

#### LIST OF PUBLICATIONS AS A PART OF DISSERTATION TOPIC

1. **Shushanyan R.**, Karapetyan H., Nadiryan E., Avtandilyan N., Grigoryan A., Karapetyan A. (2025), Tissue remodeling during high-altitude pulmonary edema in rats: Biochemical and histomorphological analysis, *Tissue & Cell*, 93, 102727. <https://doi.org/10.1016/j.tice.2025.102727>
2. **Shushanyan R.**, Grigoryan A., Nadiryan E., Karapetyan A. (2024), Acute brain edema associated with the elevated levels of oxidative stress mediators and TNF-alpha in rats: biochemical and immunohistochemical assessment, *FEBS Open Bio*, 14(2), 349-349, [doi.org/10.1002/2211-5463.13837](https://doi.org/10.1002/2211-5463.13837)
3. **Shushanyan R.** (2024), The evaluation of mast cells, TNF- $\alpha$  expression and TUNEL-positive neurons in the brain during inflammatory response induced by acute hypobaric hypoxia, *Proceedings of the YSU B: Chemical and Biological Sciences*, 58, 1 (263), 86-94. <https://doi.org/10.46991/PYSU:B.2024.58.1.086>
4. **Shushanyan R.**, Avtandilyan N., Grigoryan A., Karapetyan A. (2024), The role of oxidative stress and neuroinflammatory mediators in the pathogenesis of high-altitude cerebral edema in rats, *Respiratory Physiology & Neurobiology*, 327, 104286: [10.1016/j.resp.2024.104286](https://doi.org/10.1016/j.resp.2024.104286)
5. **Shushanyan R.**, Grigoryan A., Abgaryan T., Karapetyan A. (2023), Histological and cytochemical analysis of the brain under conditions of HH-induced oxygen deficiency in albino rats, *Acta Histochemica*, 125(8), 152114. <https://doi.org/10.1016/j.acthis.2023.152114>
6. Karapetyan M., Adamyan N., **Shushanyan R.**, Karapetyan A. (2023), Antioxidant effects of *Crataegus laevigata* on rat's brain under HH-induced oxygen deficiency, *Neurochemical Journal*, 17(3), 477-481, [doi.org/10.1134/S181971242303011X](https://doi.org/10.1134/S181971242303011X)
7. **Shushanyan R.**, Karapetyan A., Grigoryan A. (2023), Assessment of NO level and histological alterations in the rats brain during high altitude cerebral edema induced by HH, 2023, *FEBS Open Bio*, 13(S2), 112-112, <https://doi.org/10.1002/2211-5463.13646>
8. **Shushanyan R.**, Grigoryan A., Karapetyan A. (2022), Hypobaric hypoxia induces histomorphological alterations in the different parts of the rat's brain, *Proceedings of the YSU B: Chemical and Biological Sciences*, 56, 3(259), 266-274, <https://doi.org/10.46991/PYSU:B/2022.56.3.266>

## ՇՈՒՇԱՆՅԱՆ ՌՈՒԶԱՆՆԱ ԱՐՄԵՆԻ

### ԱՌՆԵՏՆԵՐԻ ՈՐՈՇ ՕՐԳԱՆՆԵՐԻ ՄՈՐՖՈՅՈՒԿՑԻՈՆԱԼ ՓՈՓՈԽՈՒԹՅՈՒՆՆԵՐԻ ԳՆԱՀԱՏՈՒՄԸ ՍՈՒՐ ՀԻՊՈՒՄԱՐԻԿ ՀԻՊՕՔՄԻԱՅԻ ՊԱՅՄԱՆՆԵՐՈՒՄ

#### Ամփոփագիր

**Հանգուցային բառեր՝** *գլխուղեղի այտուց, թոքային այտուց, արյունատղեղային պատնեշ, ավվեռյար-մազանոթային պատնեշ, հիպոբարիկ հիպոքսիա, օքսիդատիվ սթրես, արգինազ, ազոտի օքսիդ, ռեդօքս հավասարակշռություն, ՍՕԴ, կատալազ, լակտատդեհիդրոգենազ, նեյրոբոքոքում, ՈՒՆԳ-α, ֆիբրոզ, պարարտ բջիջներ:*

Հիպոբարիկ հիպոքսիան, որը բնութագրվում է ցածր բարոմետրիկ ճնշմամբ և թթվածնի սուր անբավարարությամբ, մեծ վտանգ է ներկայացնում գլխուղեղի և թոքերի այտուցի զարգացման համար՝ փոխելով դրանց կառուցվածքային և գործառական առանձանահատկությունները: Վերջիններս մեծ բարձրություններում չլիմատիզացված անհատների համար պոտենցիալ մահացու խանգարումներ են, որոնք հրահրում են բորբոքային ռեակցիա և հանգեցնում գլխուղեղում և թոքերում ռեդօքս հոմեոստազի զգալի փոփոխությունների, ինչն ի վերջո, բերում է նեյրոնների և ավվեռյար բջիջների մահվան: Հիպոբարիկ հիպոքսիան նպաստում է օքսիդատիվ սթրեսի զարգացմանը այս օրգաններում և ազդում տարբեր կենսամոլեկուլների այդ թվում՝ լիպիդների, սպիտակուցների և ԴՆԹ-ի վրա:

Այս հետազոտության նպատակն է եղել՝ գնահատել գլխուղեղի և թոքերի այտուցի զարգացման պաթոգենեզի հիմքում ընկած մեխանիզմները և դրանցում ներգրավված տարբեր կենսամոլեկուլների դերը: Սույն հետազոտության շրջանակներում ուսումնասիրվել է գլխուղեղի, թոքերի և ծայրամասային արյան բջիջների մորֆոֆունկցիոնալ փոփոխությունները սուր հիպոբարիկ հիպոքսիայի ազդեցության պայմաններում (7620մ, 24-ժամ տևողությամբ)՝ կիրառելով հյուսվածաբանական, կենսաքիմիական և ֆյուրերեստային մեթոդներ: Գնահատվել են նեյրոնների և ավվեռյար բջիջների ապոպտոտիկ և դրանցում ՈՒՆԳ-α-ի ակտիվության, ինչպես նաև պարարտ բջիջների քանակության փոփոխությունները թոքերում և գլխուղեղում՝ որպես բորբոքման մեդիատորներ: Գնահատվել է արգինազի, ազոտի օքսիդի և լիպիդների պերօքսիդացման վերջնարդյունք՝ մալոնդիալդեհիդի, հակաօքսիդանտանային համակարգի մի քանի ֆերմենտների ակտիվության փոփոխությունները սուր հիպոբարիկ հիպոքսիայի ազդեցությունի հետո:

Հետազոտության արդյունքները ցույց են տվել, որ գլխուղեղի պարենխիմայում և թոքերում պարարտ բջիջների, ինչպես նաև ՈՒՆԳ-α-դրական բջիջների քանակը մեծացել է, ինչը վկայում է բորբոքային գործընթացների առկայության մասին: Գլխուղեղի որոշ բաժիններում (հիպոկամպ, ցերեբրալ կորտեքս) դիտվել են հիպերքրոմատիզացված, վակուլիզացված (այտուց), կարիոպիկնոզով նեյրոններ, գերարյունացված անոթներ, փոքր հեմոռագիկ օջախներ և ապոպտոզի ենթարկված նյարդային բջիջներ: Կեղևում և

հիպոկամպում հայտնաբերվել են բազմաթիվ CR-դրական բջիջներ: Թոքերում մորֆոլոգիայի փոփոխության հետազոտության արդյունքում ցույց է տրվել, որ սուր հիպոքսիկ հիպոքսիայի ազդեցությունից հետո թոքային հյուսվածքում դիտվել են էդեմատոզ փոփոխություններ, բորբոքային ինֆիլտրատներ, արյունազեղումներ և ավելոյալ հեղուկի մեծածավալ կուտակումներ: Ուսումնասիրության արդյունքում պարզ է դարձել, որ վերոնշյալ օրգաններում փոխվել է նաև ռեդօքս հավասարակշռությունը, որն ուղեկցվել է հակաօքսիդանտային համակարգի և օքսիդատիվ սթրեսին մասնակցող կենսամոլեկուլների քանակական փոփոխություններով: Վերջինս վկայում է գլխուղեղի և թոքերի սուր այտուցի զարգացման մեջ ուսումնասիրված կենսամոլեկուլների և բջիջների կարևոր դերի մասին: Ավելին, հետազոտությամբ ցույց է տրվում ՈՒՆԳ- $\alpha$ -ի և պարարտ բջիջների ներգրավվածությունը արյունառեղադային և ավելոյալ-մազանոթային պատնեշի խանգարման գործում: Այս ուսումնասիրությունը թույլ է տալիս է առավել համապարփակ պատկերացում կազմել գլխուղեղի և թոքերի սուր այտուցի պաթոգենեզի և դրա հիմքում առկա բջջային և մոլեկուլային մեխանիզմների մասին, որում ուսումնասիրված կենսաբանական մոլեկուլները և բջիջները ունեն մեծ նշանակություն՝ որպես ռեդօքս հոմեոստազի և բորբոքային ռեակցիաների կարևոր մոդուլատորներ:

## ШУШАНЯН РУЗАННА АРСЕНОВНА

### ОЦЕНКА МОРФОФУНКЦИОНАЛЬНЫХ ИЗМЕНЕНИЙ НЕКОТОРЫХ ОРГАНОВ КРЫС ПРИ ОСТРОЙ ГИПОБАРИЧЕСКОЙ ГИПОКСИИ РЕЗЮМЕ

**Ключевые слова:** *отек мозга, отек легких, гематоэнцефалический барьер, альвеоларно-капиллярный барьер, гипобарическая гипоксия, окислительный стресс, аргиназа, оксид азота, окислительно-восстановительный баланс, СОД, каталаза, лактатдегидрогеназа, нейровоспаление, ФНО- $\alpha$ , фиброз, тучные клетки.*

Гипобарическая гипоксия, обусловленная низким атмосферным давлением и острым дефицитом кислорода, представляет значительный риск для развития отёка мозга и лёгких, а также приводит к изменениям их структурных и функциональных характеристик. Эти изменения могут оказаться потенциально смертельными для неакклиматизированных людей на больших высотах, провоцируя воспалительные реакции и нарушая окислительно-восстановительный гомеостаз в мозге и лёгких, что в конечном итоге может привести к гибели нейронов и альвеоларных клеток. Гипобарическая гипоксия способствует увеличению окислительного стресса в этих органах и оказывает влияние на различные биомолекулы, включая липиды, белки и ДНК.

Целью данного исследования было изучение механизмов патогенеза отеков головного мозга и лёгких, а также роли различных биомолекул, вовлечённых в этот процесс. В ходе эксперимента с использованием гистологических, биохимических и флуоресцентных методов были исследованы морфофункциональные изменения в мозге, лёгких и периферической крови при остром воздействии гипобарической гипоксии (на высоте 7620м в течение 24 часов). Результаты показали, что происходят изменения в апоптотической активности нейронов и альвеолярных клеток, а также в количестве тучных клеток в лёгких и мозге, которые выступают в роли медиаторов воспаления. Были оценены изменения активности аргиназы, оксида азота, конечного продукта перекисного окисления липидов – малонового диальдегида, а также различных ферментов антиоксидантной системы после воздействия острого гипоксического состояния.

Исследование выявило увеличение численности тучных клеток в тканях мозга и лёгких, а также клеток, позитивных к ФНО- $\alpha$ , что свидетельствует о наличии воспалительных процессов. В отдельных участках мозга (гиппокампе, коре) наблюдались гиперхроматизированные и вакуолизированные нейроны с явлениями кариопикноза, а также увеличенные сосуды, мелкие геморрагические очаги и апоптоз нервных клеток. В коре головного мозга и гиппокампе было обнаружено множество CR-позитивных клеток. Гистоморфологическое исследование лёгких показало, что воздействие острого гипобарического стресса привело к отечным изменениям, воспалительным инфильтратам, кровоизлияниям и значительному накоплению альвеолярной жидкости. В результате исследования также было установлено, что в этих органах изменяется окислительно-восстановительный баланс, что сопровождается количественными изменениями в антиоксидантной системе и биомолекулах, вовлечённых в окислительный стресс. Это подчеркивает важную роль изученных биомолекул и клеток в развитии острого отека мозга и лёгких. Более того, результаты показывают участие провоспалительных цитокинов, особенно ФНО- $\alpha$ , и тучных клеток в нарушении гематоэнцефалического и альвеолярно-капиллярного барьеров. Данное исследование предоставляет более полное понимание патогенеза острого отека мозга и лёгких и сопутствующих клеточных и молекулярных механизмов, где изученные биомолекулы и клетки играют ключевую роль как важные модуляторы окислительно-восстановительного гомеостаза и воспалительных реакций.

